LASER GYROSCOPES

PACS numbers: 42.60.DA; 07.07.Df; 42.79.Gn
DOI: 10.1070/QE2014v044n12ABEH015396

On the possibility of using the phase characteristic of a ring interferometer in microoptical gyroscopes

V.Yu. Venediktov, Yu.V. Filatov, E.V. Shalymov

Abstract. **The prototype schemes of a microoptical gyroscope (MOG) developed to date on the basis of passive ring cavities imply the use of the amplitude characteristic only, since they operate using the dip in the transmission coefficient. We have analysed the possibility of creating a MOG, in which the phase characteristic is used as well. The phase characteristic of a ring interferometer has distinctive features in the vicinity of the cavity eigenfrequencies, which may be used to determine the angular velocity. A method for the angular velocity determination using both the phase and the amplitude characteristics of the interferometer is considered.**

Keywords: *phase characteristic, interferometer, microoptical gyroscope.*

1. Introduction

The demand for cheap and compact sensitive elements for inertial systems of orientation and navigation led to the appearance of micromechanical gyroscopes, actively developed at the present time. However, the sensitivity of modern micromechanical gyroscopes to linear accelerations, vibrations and shock impacts limits the field of their application (see, e.g., [1, 2]). At the same time the development of optical (laser and fibre optical) gyroscopes continues, which are characterised by high accuracy, are practically insensitive to linear accelerations and operate in a wide range of velocities [3, 4]. The main drawbacks of optical gyroscopes are their high cost and large dimensions.

The progress of integral optics laid the grounds for the studies aimed at essential reduction of the overall size and cost of optical gyroscopes. The most interesting version of the optical gyroscope from the point of view of miniaturisation is the microoptical gyroscope (MOG) with a passive ring cavity on the basis of buried waveguides in planar implementation [5, 6].

To date all known MOG prototypes imply the use of the amplitude characteristic (since they operate using the peak or dip of the transmission coefficient) of the ring interferometer for determining the difference of its cavity eigenfrequencies, proportional to the angular velocity of rotation. In the present paper we consider the principle of the MOG operation, based on the measurement of the transmission coefficient. The possibility of designing a MOG, in which the phase characteristic is used as an alternative to using the amplitude characteristic solely is analysed, and a method of angular velocity determination using both the phase and the amplitude characteristic of the interferometer is described.

V.Yu. Venediktov V.I. Ulyanov (Lenin) Saint Petersburg State Electrotechnical University LETI, ul. Prof. Popova 5, 197376 St. Petersburg, Russia; Department of Physics, Saint-Petersburg State University, ul. Ul'yanovskaya 3, Staryi Petergof, 198504 St. Petersburg, Russia; e-mail: vlad.venediktov@mail.ru;
Yu.V. Filatov, E.V. Shalymov V.I. Ulyanov (Lenin) Saint Petersburg State Electrotechnical University LETI, ul. Prof. Popova 5, 197376 St. Petersburg, Russia; e-mail: yvfilatov@mail.eltech.ru

Received 29 January 2014; revision received 11 April 2014
Kvantovaya Elektronika **44** (12) 1145–1150 (2014)
Translated by V.L. Derbov

2. Principle of MOG operation

Consider the principle of MOG operation by the example of the scheme with a passive ring cavity (PRC), presented in Fig. 1.

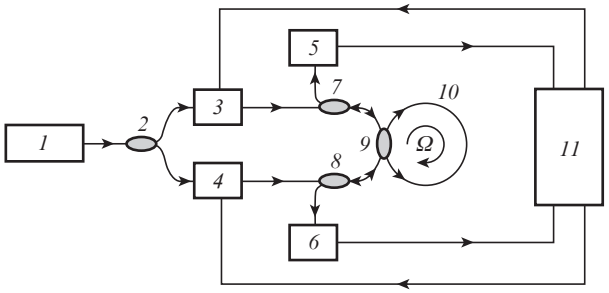

Figure 1. Functional diagram of a MOG with the PRC (see the text for notations).

Radiation from laser (*1*) is split by the Y-coupler (*2*) into two channels. The phase modulators (*3*) and (*4*) change the frequencies of the signals transmitted through them. The system includes three directional couplers (*7*, *8*, *9*). By means of coupler (*9*) radiation from both channels is introduced into the cavity of the ring interferometer (*10*) (ring waveguide a few centimetres in diameter) in two opposite directions (clockwise and counter-clockwise). Via couplers (*7*, *8*, *9*) radiation from the PRC is directed to photodetectors (*5*) and (*6*), the signals from which then arrive at the computing system (*11*).

If the MOG does not rotate with respect to an inertial coordinate system, then the intensities of the radiation at detectors (*5*) and (*6*) (I_1 and I_2, respectively) vary depending on its frequency as shown in Fig. 2. In this case the positions of the dips in the amplitude characteristic coincide with the eigenfrequencies (resonance frequencies) of the PRC f_m. If the laser radiation frequency is not equal to the PRC eigenfrequency, then radiation is practically not absorbed by the ring waveguide and reaches the photodetectors. If the radiation frequency is a resonance one, then radiation is absorbed by

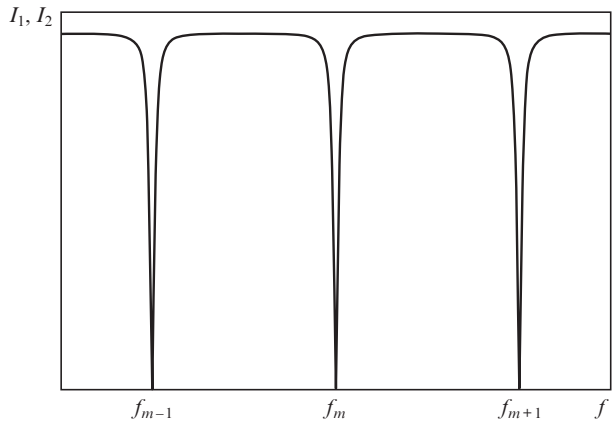

Figure 2. Radiation intensity at the photodetectors in the absence of MOG rotation; f_m is the resonance PRC frequency.

the ring waveguide and then dissipates in it, since the ring waveguides with the diameter of a few centimetres are usually characterised by sufficiently high losses, a few decibels per roundtrip. In the absence of MOG rotation the PRC eigenfrequencies are equal and given by the expression

$$f_m = mc/(nL), \tag{1}$$

where m is a positive integer; c is the velocity of light propagation in vacuum; n is the refractive index of the waveguide material; and L is the ring cavity perimeter.

When the MOG rotates in the plane of Fig. 1, the cavity eigenfrequencies are split due to the Sagnac effect, and the intensities of the radiation at detectors (*5*) and (*6*) depend on the frequency as shown in Fig. 3. The difference of eigenfrequencies is determined by the expression

$$f_{m\,\mathrm{ccw}} - f_{m\,\mathrm{cw}} = \frac{4S}{\lambda_m L}\Omega, \tag{2}$$

where S is the cavity area; $\lambda_m = c/f_m$; and Ω is the angular velocity of MOG rotation in the plane of Fig. 1.

In most developed MOG prototypes the computing system produces a feedback signal for modulators, tunes the frequencies in the channels to the cavity eigenfrequencies, determines the frequency difference and calculates the corresponding angular velocity, i.e., for measuring the angular velocity only the amplitude characteristic of the ring interferometer is used.

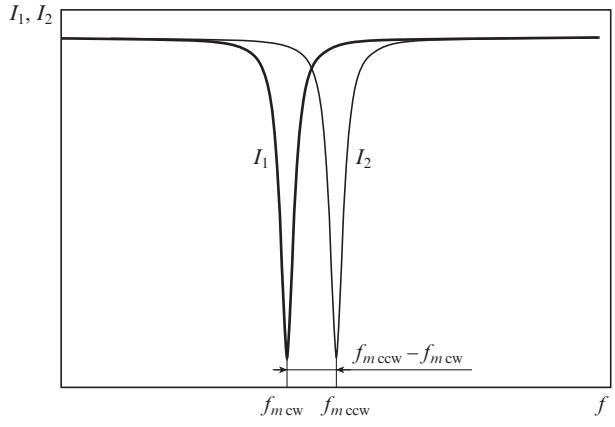

Figure 3. Radiation intensity at detectors (*5*) and (*6*) in the presence of MOG rotation; $f_{m\,\mathrm{cw}}$ and $f_{m\,\mathrm{ccw}}$ are the PRC resonance frequencies for the waves propagating clockwise and counter-clockwise, respectively.

Besides the MOG scheme considered above, which is based on a ring interferometer with one loop of optical coupling between the ring waveguide and the auxiliary one, other versions of MOG implementation exist. For example, a MOG scheme on the basis of a ring interferometer with two loops of optical coupling is known. One loop is intended for injecting radiation into the cavity, and the other one serves for radiation output. However, in this case the desing of the ring interferometer is complicated and the losses of the radiation energy are increased.

3. Model of a ring interferometer with losses

The sensitive element in the MOG is the ring interferometer. In MOGs developed at present time the ring interferometers with the cavity diameter smaller than 2 cm are used. Such an interferometer is schematically shown in Fig. 4. Radiation is injected into the interferometer via the left-hand end of the auxiliary waveguide, and is coupled out via the right-hand one [7].

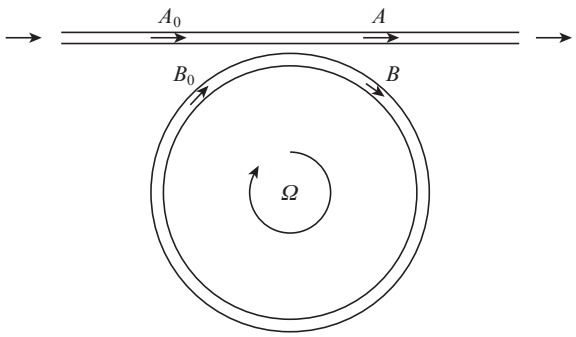

Figure 4. Schematic of the ring interferometer.

When radiation having the electric field strength A_0 propagates through the region of the auxiliary waveguide coupled to the ring cavity, a fraction of the wave energy is transferred from the auxiliary waveguide to the ring cavity. The electric field strength of this part of the wave is equal to $A_0\sqrt{K_c}$, where K_c is the energy coefficient of coupling between the auxiliary waveguide and the ring cavity. Another fraction of the initial wave stays in the auxiliary waveguide, its field strength being equal to $A_0\sqrt{1-K_c}$. When radiation having the electric field strength B_0 propagates through the region of the ring cavity, optically coupled to the auxiliary waveguide, a part of the wave stays in the cavity, and the other part is transferred to the auxiliary waveguide. The electric field strength of the wave passed to the auxiliary waveguide is equal to $B_0\sqrt{K_c}$, and for the wave left in the ring cavity it is $B_0\sqrt{1-K_c}$. Taking into account the fact that the transmission of radiation from one optically coupled waveguide to another is accompanied by the phase jump by $\pi/2$ [8], the complex field strength amplitudes of the electric field A_0, A, B_0 and B (Fig. 4) can be related by the expressions

$$A = A_0\sqrt{1-K_c} - \mathrm{i}B_0\sqrt{K_c}, \tag{3}$$

$$B = -iA_0\sqrt{K_c} + B_0\sqrt{1 - K_c}, \quad (4)$$

$$B_0 = B\exp\left(-\frac{\rho}{2}L - i\beta L\right), \quad (5)$$

where ρ is the parameter that determines the radiation power losses with $P = 1 - \exp(-\rho L)$ being the power fraction, lost during one cavity roundtrip; and β is the propagation constant.

For simplicity we neglect the losses in the auxiliary waveguide and in the optical coupler. Let us introduce the notations

$$x = \exp\left(-\frac{\rho}{2}L\right), \quad (6)$$

$$y = \sqrt{1 - K_c}, \quad (7)$$

$$\delta = \beta L = \frac{2\pi}{\lambda}N_{eff}L = \frac{\omega N_{eff}L}{c}, \quad (8)$$

where δ is the wave phase increment per one roundtrip along the cavity perimeter; N_{eff} is the effective refractive index of the waveguide; λ is the optical radiation wavelength in vacuum; and ω is the circular frequency of optical radiation.

Using Eqns (3)–(8) and performing simple transformations, we arrive at the formula for the ratio of the field strengths A and A_0:

$$\frac{A}{A_0} = \frac{y - \exp(-i\delta)}{1 - xy\exp(-i\delta)}. \quad (9)$$

It is easy to see that the energy transmission coefficient T of the ring interferometer (the ratio of intensities at the output and the input of the interferometer) is equal to the square modulus of Eqn (9), and the phase shift of the wave passed through the interferometer $\Delta\Phi$ is equal to the argument of the complex expression (9).

Figure 5 presents the dependences $T(\delta)$, calculated using expressions (6)–(9). It is seen that with the growth of K_c the depth of the transmission coefficient dip increases (Fig. 5a), and with the reduction of losses it decreases (Fig. 5b). Correspondingly, when there are no losses in the cavity, the amplitude characteristic demonstrates no dips at the eigenfrequencies of the cavity (Fig. 5b). The dips of the transmission coefficient correspond to the condition of resonance, when the phase shift equals $\delta = 2\pi m$ (the path length of the radiation in the cavity is an integer multiple of the wavelength), where m is an integer.

From Fig. 6 it is seen that the slope of the phase characteristic and its maximal value increase both with the reduction of losses and with the growth of K_c. If the phase increment per cavity roundtrip, caused by the change of the radiation frequency or the cavity perimeter, is equal to δ, then the $\Delta\Phi$ value varies following a periodical law within the interval, the width of which is determined by the level of losses and the value of the coupling coefficient (the maximal interval is $[-\pi; \pi]$). At resonance ($\delta = 2\pi m$) the slope of the phase characteristic is maximal and $\Delta\Phi = 0$. In the vicinity of a resonance frequency the phase characteristic is close to linear. The characteristic possessing such properties seems attractive for using in MOGs for determination of resonance frequencies.

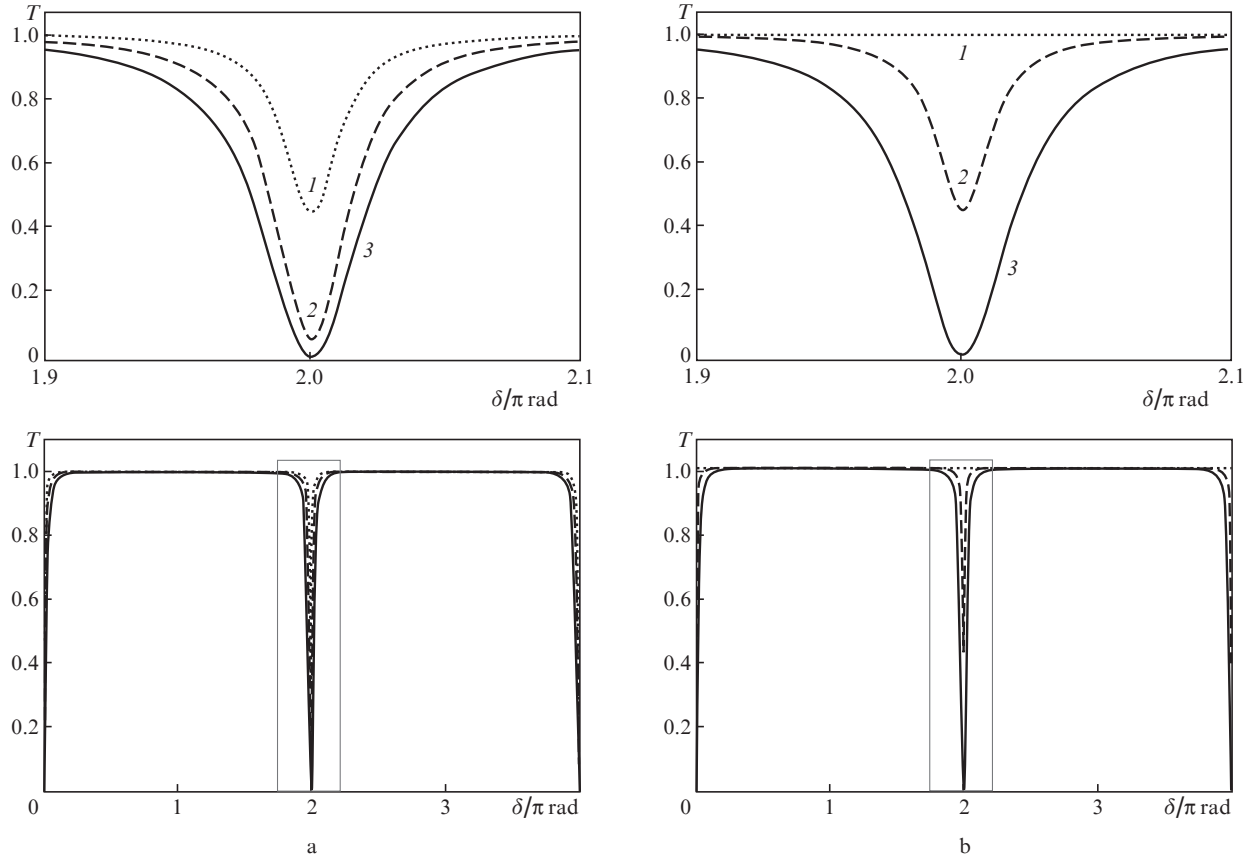

Figure 5. Transmission coefficients of the interferometer, calculated (a) for K_c = (*1*) 0.01, (*2*) 0.03 and (*3*) 0.06, P = 5% and (b) for P = (*1*) 0, (*2*) 1% and (*3*) 6%, $K_c = 0.05$.

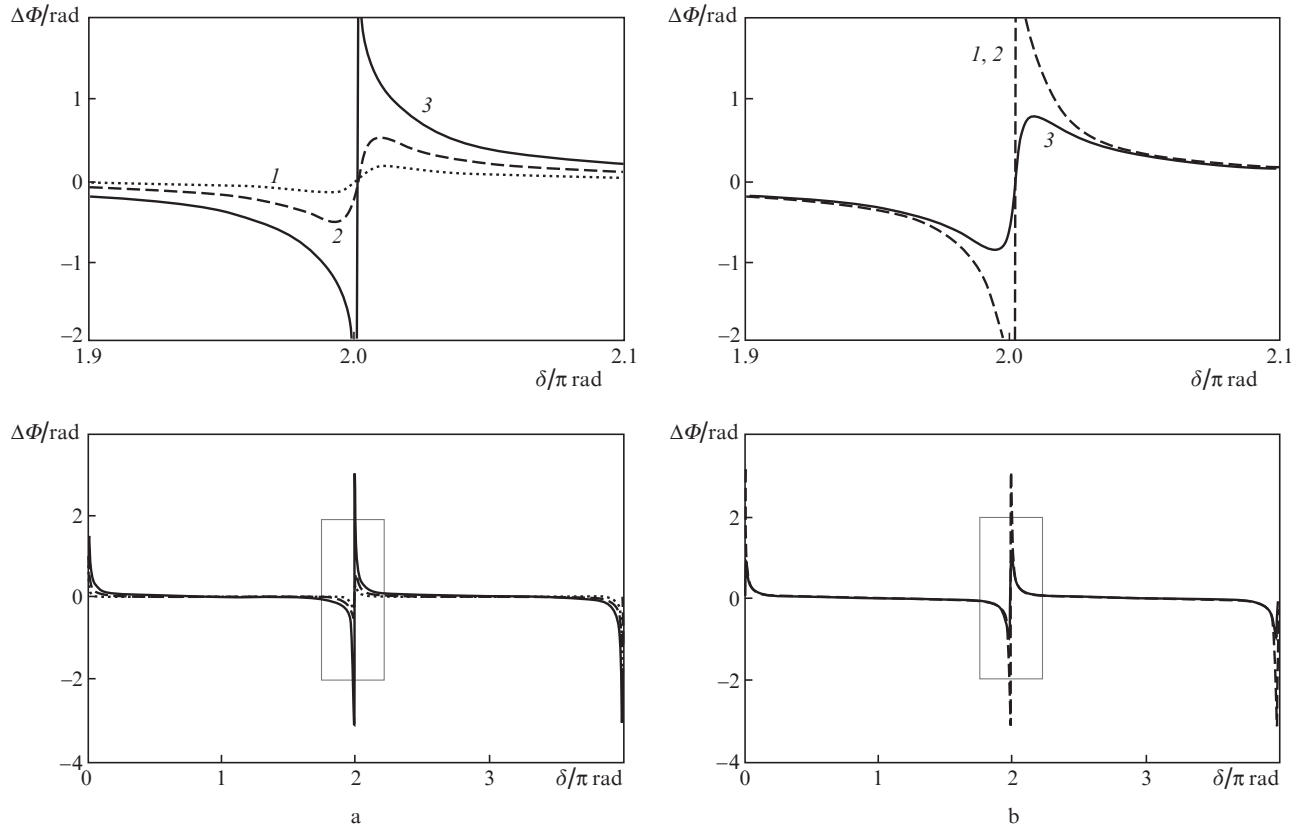

Figure 6. Phase shifts of the wave passing the interferometer, calculated (a) for K_c = (*1*) 0.01, (*2*) 0.03 and (*3*) 0.06, P = 5% and (b) for P = (*1*) 0, (*2*) 1% and (*3*) 6%, K_c = 0.05.

As already mentioned above, the rotation of the ring interferometer gives rise to the splitting of the amplitude characteristic for the waves, travelling around the cavity in opposite directions (see Fig. 3). Similar splitting occurs with the phase characteristic of the ring interferometer (Fig. 7). Figure 7 presents the frequency dependence of the phase shifts $\Delta\Phi_1$ and $\Delta\Phi_2$ accumulated during the cavity roundtrip for the waves travelling in the clockwise and counter-clockwise directions, respectively. Such splitting of the phase characteristic occurs for the clockwise rotation of the interferometer. The difference of eigenfrequencies is proportional to the velocity of rotation [see Eqn (2)].

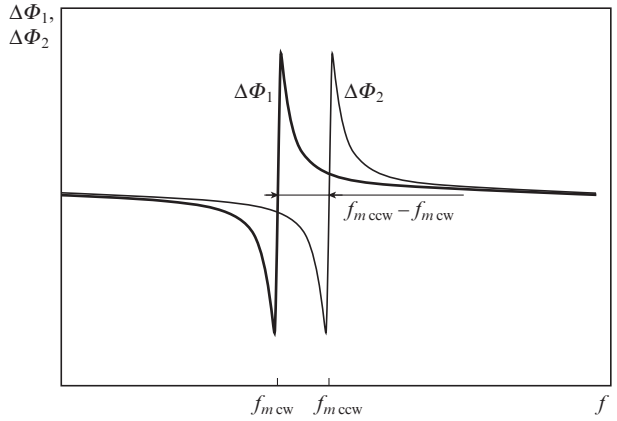

Figure 7. Phase characteristic splitting in the ring interferometer due to its rotation.

4. Use of the phase characteristic of the ring interferometer in a MOG

All MOG prototypes known to date imply the use of the amplitude characteristic only (see, e.g., [9–12]) for determining the difference of the cavity eigenfrequencies, proportional to the velocity of its rotation. The results of the analysis of ring interferometer characteristics show that the phase characteristic possesses distinctive features in the vicinity of the cavity eigenfrequencies. It is not possible to perform a direct measurement of the optical signal phase; however, the information about it may be obtained from the interference patterns, as, e.g., in the case of fibre-optical gyroscopes [4]. It is possible to design a MOG, in which only the phase characteristic is used to determine the difference of the interferometer cavity eigenfrequencies, as well as a MOG, in which both the phase and the amplitude characteristic of the interferometer is used. We continue the studies in both directions. As a result of these studies, the method for determining the angular velocity using the phase and the amplitude characteristic of the ring cavity was developed. Consider this method by the example of the device operation, implementing it.

The schematic of the device is shown in Fig. 8. It consists of laser (*1*), optical couplers (*2*, *5*, *7*, *9*), phase modulators (*3*, *4*), photodetectors (*6*, *8*) and ring interferometer (*10*), connected by optical waveguides, and computing system (*11*). Laser radiation is split by the optical coupler (*2*) into two waves B1 and B2 (from the point of view of high-precision angular velocity measurement it is optimal to split the beam into two waves of equal intensity). Then, the waves B1 and B2 pass through phase modulators (*3*) and (*4*) controlled by the

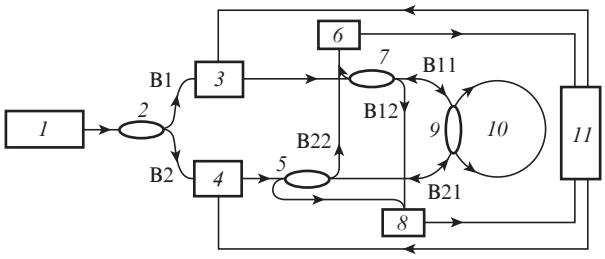

Figure 8. Functional diagram of the MOG using both the phase and the amplitude characteristic of the ring interferometer (see notations in the text).

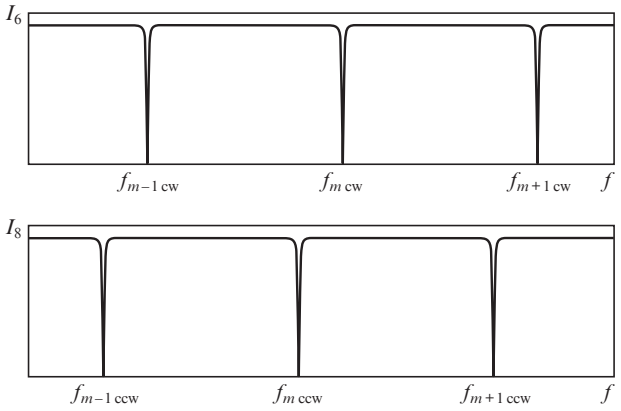

Figure 9. Dependences of the radiation intensity incident on photodetectors (*6*) and (*8*) on the frequency for $K_c = 0.05$ and $P = 0$.

computing system (*11*). These modulators provide a periodic linear variation of frequency. The resulting frequency-modulated waves are split by optical couplers (*7*) and (*5*). The wave B1 is split into the waves B11 and B12, and the wave B2 is split into the waves B21 and B22. The reference waves B12 and B22 are guided to photodetectors (*6*) and (*8*), and the waves B11 and B21 are injected into the ring interferometer (*10*), in which their parameters (intensity and phase) are changed. In the interferometer cavity the input and output of radiation is provided by means of the same optical coupling loop, implemented using the directional optical coupler (*9*). From the interferometer the output signals B11 and B21, carrying the measurement information, are guided to photodetectors (*6*) and (*8*) via couplers (*7*) and (*5*). Thus, photodetector (*6*) records the interference pattern of the waves B11 and B12, while photodetector (*8*) records that of the waves B21 and B22. For simplicity, let us consider the case when the difference of the optical path lengths of the reference signals and the signals carrying the measurement information is equal to an integer number of wavelengths λ_m. For this case the dependences of the optical radiation intensity, incident on photodetectors (*6*) and (*8*) (I_6 and I_8, respectively), on the radiation frequency are presented in Fig. 9.

The minima of the optical radiation intensity correspond to the cavity eigenfrequencies $f_{m\,\mathrm{cw}}$ and $f_{m\,\mathrm{ccw}}$ (for the waves, travelling in the cavity clockwise and counter-clockwise, respectively). Using the minima of the signals from the photodetectors, the computing system (*11*) determines the eigenfrequencies, and then their difference f, proportional to the angular velocity. When the difference of the optical path lengths between the reference signals and the signals carrying the measurement information is not an integer number of wavelengths λ_m, the shape of the dependences presented in Fig. 9 changes. Nevertheless, for any difference of the optical path lengths it remains possible to determine the resonance frequencies using characteristic variations of the intensity of the radiation, incident of the photodetectors, near the cavity eigenfrequencies.

The MOG sensitivity depends on the level of losses in the cavity of the ring interferometer, namely, the lower the losses, the higher the sensitivity [2]. As already mentioned above, in the absence of losses in the cavity of the ring interferometer the amplitude characteristic has no dips at the cavity eigenfrequencies, i.e., in the absence of losses it is impossible to determine the angular velocity using the dips in the amplitude characteristic. It is worth noting, that in real ring interferometers the losses are always present ($P \neq 0$). However, the losses can be compensated for by implementing gain inside the planar waveguide [9]. Using the phase characteristic in the MOG makes it possible to determine the angular velocity even in the case of full compensation of losses (Fig. 9).

When the losses in the cavity of the ring interferometer are relatively low, the combined use of the amplitude and the phase characteristic allows one to increase the dip depth and

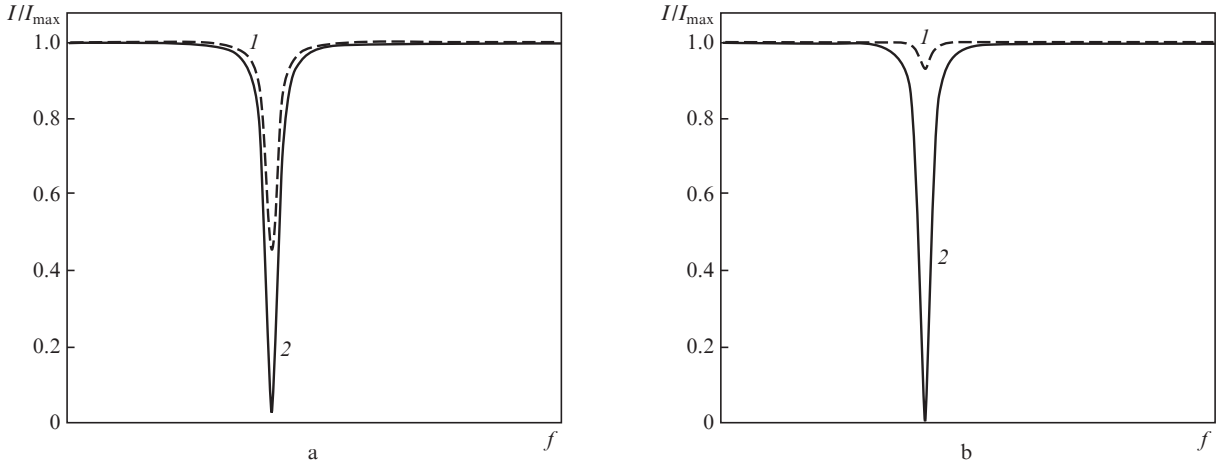

Figure 10. Relative intensity of radiation incident on the MOG photodetector at (a) $K_c = 0.05$, $P = 1\%$ and (b) $K_c = 0.05$, $P = 0.1\%$ for the MOG using only the amplitude characteristic of the ring interferometer (*1*), and using both the amplitude and the phase characteristic (*2*).

the slope of the output characteristic (Fig. 10). At $K_c = 0.05$ and $P = 1\%$ the maximal slope of the MOG output characteristic in the case of using both the phase and the amplitude characteristic of the ring interferometer exceeds that of the MOG using the amplitude characteristic only by almost two times, and with the losses reduced to 0.1% – by more than 13 times.

5. Conclusions

In the present paper we consider the principle of MOG operation based on the use of the amplitude characteristic of the ring cavity. The phase characteristic of a ring interferometer has distinctive features near the cavity eigenfrequencies, which allow it to be used for determining the rotation velocity. We also consider an example of implementation of the angular velocity measuring method using the phase and the amplitudes characteristic of the ring interferometer in combination. In the future we plan to continue the development of MOGs using the phase characteristic.

Acknowledgements. Yu.V. Venediktov is an executor of the project 'Organisation of Scientific Research' of the base part of the State Task from the Ministry of Education and Science of the Russian Federation. The modelling of ring interferometer was carried out under the support from the Russian Scientific Foundation (Grant No. 14-19-00693).

References

1. Schmidt G.T., in *Advances in Navigation Sensors and Integration Technology* (NATO RTO Lecture Series, 2004).
2. Boronakhin A.M., Luk'yanov D.P., Filatov Yu.F. *Opticheskiye i mikromekhanicheskiye inertsial'nye pribory* (Optical and Micromechanical Inertial Instruments) (St. Petersburg: Izd-vo 'Elmor', 2008).
3. Chow W.W., Gea-Banacloche J., Pedrotti L.M., Sanders V.E., Schleich W., Scully M.O. *Rev. Mod. Phys*., **57**, 61 (1985).
4. Lefèvre H. *The Fiber-Optic Gyroscope* (Norwood, USA, Artech House Inc., 1993).
5. Ford C., Ramberg R., Johnson K. *IEEE Aerosp. Electron. Syst. Mag.*, №12, 33 (2000).
6. Li G., Winick K.A., Youmans B. *Proc. ION 60th Annual Meeting* (Dayton, Ohio, 2004).
7. Bismuth J., Revol P., Valette S. *Electron. Lett*., **27**, 722 (1991).
8. Nikonorov N.V., Shaddarov S.M. *Volnovodnaya fotonika. Uchebnoye posobiye, kurs lektsiy* (Waveguide Photonics. A Tutorial Lecture Course) (St. Petersburg: SPbGU ITMO, 2008).
9. Hsien-kai Hsiao, Winick K.A. *Opt. Express*, **15** (26), 17783 (2007).
10. Terrel M., Digonnet M.J.F., Fan Sh. *Laser Photonics Rev*., **3** (5), 452 (2009).
11. Wang X., He Z., Hotate K. *Proc. SPIE Int. Soc. Opt. Eng.*, **7314**, 731402 (2009).
12. Mao H., Ma H., Jin Z. *Opt. Express*, **19** (5), 4632 (2011).